

PAPER

Unconventional quantum Hall effect in Floquet topological insulators

To cite this article: M Tahir *et al* 2016 *J. Phys.: Condens. Matter* **28** 385302

View the [article online](#) for updates and enhancements.

Related content

- [Optical conductivity of topological insulator thin films in a quantizing magnetic field](#)
A Ullah and K Sabeeh
- [Quantum anomalous Hall effect in time-reversal-symmetry breaking topological insulators](#)
Cui-Zu Chang and Mingda Li
- [Thermoelectric properties of an ultra-thin topological insulator](#)
SK Firoz Islam and T K Ghosh

Unconventional quantum Hall effect in Floquet topological insulators

M Tahir¹, P Vasilopoulos¹ and U Schwingenschlög²

¹ Department of Physics, Concordia University, Montreal, QC H3G 1M8, Canada

² King Abdullah University of Science and Technology (KAUST), Physical Science and Engineering Division (PSE), Thuwal 23955-6900, Saudi Arabia

E-mail: udo.schwingenschlogl@kaust.edu.sa, m.tahir06@alumni.imperial.ac.uk and p.vasilopoulos@concordia.ca

Received 8 April 2016, revised 6 July 2016

Accepted for publication 6 July 2016

Published 27 July 2016



Abstract

We study an unconventional quantum Hall effect for the surface states of ultrathin Floquet topological insulators in a perpendicular magnetic field. The resulting band structure is modified by photon dressing and the topological property is governed by the low-energy dynamics of a single surface. An exchange of symmetric and antisymmetric surface states occurs by reversing the light's polarization. We find a novel quantum Hall state in which the zeroth Landau level undergoes a phase transition from a trivial insulator state, with Hall conductivity $\sigma_{yx} = 0$ at zero Fermi energy, to a Hall insulator state with $\sigma_{yx} = e^2/2h$. These findings open new possibilities for experimentally realizing nontrivial quantum states and unusual quantum Hall plateaus at $(\pm 1/2, \pm 3/2, \pm 5/2, \dots)e^2/h$.

Keywords: Floquet, quantum Hall effect, topological insulator

(Some figures may appear in colour only in the online journal)

In the regime of the integral quantum Hall effect (IQHE) for conventional, two-dimensional (2D) systems, e.g. in a GaAs/AlGaAs heterostructure, the Hall conductivity takes the values $2(n+1)e^2/h = (2, 4, 6, \dots)e^2/h$, where h is the Planck constant, e the electron charge, and n an integer. In graphene though the IQHE plateaus appear at $4(n+1/2)e^2/h = (\pm 2, \pm 6, \pm 10, \dots)e^2/h$ [1], and the 'half integer' aspect is hidden under the 4-fold degeneracy associated with the spin and valley degrees of freedom [2]. More recently, the IQHE has been assessed for silicene [3] and MoS₂ [4] in which the spin-orbit interaction rearranges, as in 2D systems [5], the Landau levels (LLs) in two groups and the plateaus appear at integer values of e^2/h due to a double degeneracy $(\pm 0, \pm 1, \pm 2, \pm 4, \pm 6, \dots)$. In topological insulators (TIs) electrons on both the top and bottom surfaces contribute to the Hall conductivity and its plateaus, due to the surface degeneracy, having heights $2(n+1/2)e^2/h = (\pm 0, \pm 1, \pm 3, \pm 5, \dots)e^2/h$ [6–8]. Though the quest for a genuine 'half-integer' QHE is long, a QHE like $(n+1/2)e^2/h = (\pm 0, \pm 1/2, \pm 3/2, \pm 5/2, \dots)e^2/h$ without any degeneracy prefactor has not been observed. Then one wonders whether a 'half-integer' QHE is possible in TIs by breaking their surface degeneracy.

TIs, well established theoretically [9] and experimentally [10], are a state of matter, that cannot appear in normal 2D systems with time-reversal symmetry [11]. They exhibit exotic properties such as disorder-protected conducting surface states, a single Dirac cone, quantum phase transitions [12, 13], etc. These findings generated a strong interest in TIs that was further intensified by their potential applications in quantum computing [14], optical devices [15], terahertz detectors [16], etc.

More recently, the surface states of TIs driven by circularly polarized *off-resonant* light have become a subject of strong interest [17–20]. TIs driven by external time-periodic perturbations are known as Floquet TIs (FTIs). For such systems it is convenient to use the Floquet theory [18]. In the appropriate frequency regime the *off-resonant* light cannot generate real photon absorption or emission due to energy conservation. Accordingly, it does not directly excite electrons but instead modifies the electron band structure through second-order virtual-photon absorption processes. Averaged over time these processes result in an effective static alteration of the band structure. Illuminating, e.g. graphene or silicene with *off-resonant* light generates a Haldane-type gap [21].

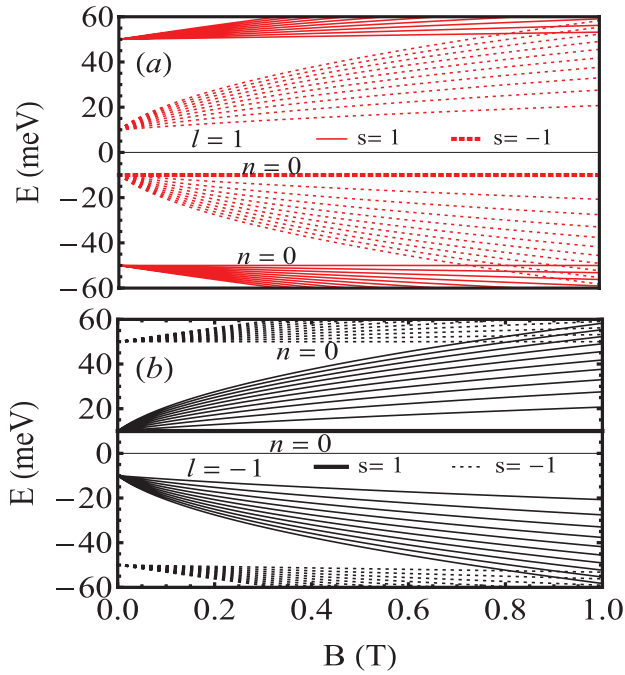


Figure 1. Energy spectrum versus magnetic field B . The symmetric (solid curves) and antisymmetric (dashed curves) surface states are shown for right-handed (a) and (b) left-handed light with $\Delta_h = 20$ meV and $\Delta_\Omega = 30$ meV. Note that the first two $n = 0$, B -independent LLs (thick lines) are in the valence (conduction) band for right-handed (left-handed) light.

Floquet bands were first realized in photonic crystals [22] and have been verified by recent experiments on the surface states of FTIs [23, 24]. These first studies of *off-resonant* light were limited to the band structure of FTIs and differ from many optical effects in TIs [15]. Also, no magnetic field was involved in these experiments.

In this work we identify a novel quantum Hall state of ultrathin FTIs in a magnetic field when their surface degeneracy is broken due to an *off-resonant* light. We evaluate their band structure and the longitudinal and Hall conductivities using linear response theory [25, 26].

Model formulation

We consider surface states of ultrathin TIs in the (x, y) plane in the presence of circularly polarized *off-resonant* light [18] and hybridization [27] between the top and bottom surface states. Extending the 2D Dirac-like Hamiltonian [18, 28] by including an external perpendicular magnetic field B gives

$$H_s^l = v_F(\sigma_x \Pi_y - \sigma_y \Pi_x) + s\Delta_h \sigma_z + l\Delta_\Omega \sigma_z, \quad (1)$$

where $s = +/-$ is for symmetric/antisymmetric surface states, $l = +/-$ for right-/left-handed circularly polarized *off-resonant* light, $(\sigma_x, \sigma_y, \sigma_z)$ the Pauli matrices and v_F the Fermi velocity. Δ_h is the hybridization energy between the top and bottom surface states that, depending on the thickness, varies from 20 meV to 120 meV [29]. $\Delta_\Omega = e^2 v_F^2 \hbar^2 A_0^2 / \hbar^3 \Omega$ is the mass term induced by the *off-resonant* light with amplitude E_0 , Ω the light's frequency, and $A_0 = E_0 / \Omega$. It breaks the

time-reversal symmetry and its value is about 50 meV [23, 24]. $\mathbf{\Pi} = \mathbf{p} + e\mathbf{A}$ is the 2D canonical momentum with vector potential $\mathbf{A} = (0, Bx, 0)$, diagonalizing the Hamiltonian (1) gives the eigenvalues

$$E_{n,s}^{\lambda,l} = \lambda[\hbar^2 \omega_c^2 n + \Delta_{s,l}^2]^{1/2}, \quad E_{0,s}^{0,l} = -\Delta_{s,l}, \quad (2)$$

where $\lambda = \pm 1$ represents the electron/hole states, $\omega_c = v_F \sqrt{2eB/\hbar}$, and $\Delta_{s,l} = l\Delta_\Omega + s\Delta_h$. The corresponding normalized eigenfunctions are

$$\Psi_{n,s}^{\lambda,l} = \frac{e^{ik_y y}}{\sqrt{L_y}} \begin{pmatrix} C_{n,s}^{\lambda,l} \phi_{n-1} \\ D_{n,s}^{\lambda,l} \phi_n \end{pmatrix}, \quad \Psi_{0,s}^{0,l} = \frac{e^{ik_y y}}{\sqrt{L_y}} \begin{pmatrix} 0 \\ \phi_0 \end{pmatrix}, \quad (3)$$

where $C_{n,s}^{\lambda,l} = [(E_{n,s}^{\lambda,l} + \Delta_{s,l})/2E_{n,s}^{\lambda,l}]^{1/2}$, $D_{n,s}^{\lambda,l} = [(E_{n,s}^{\lambda,l} - \Delta_{s,l})/2E_{n,s}^{\lambda,l}]^{1/2}$; ϕ_n are the harmonic oscillator functions. Notice that equation (1) does not contain the Zeeman term $g s_z B$. We neglect it, because we consider only weak B fields ≤ 1 T, see figure 1. For a g factor as large as 20 the Zeeman energy at $B = 1$ T is 0.58 meV and much smaller than all other energies.

A close inspection of equation (2) shows that we have a gapped Dirac spectrum, with gap Δ_h , and electron-hole symmetry for zero *off-resonant* light, $\Delta_\Omega = 0$. For $\Delta_\Omega > \Delta_h > 0$, the eigenvalues of equation (2) show a \sqrt{B} dependence and the LLs split, see figure 1. We find an exchange of the symmetric (solid curves) and antisymmetric (dotted curves) surface states by changing the light's polarization from right (red curves) to left (black curves). The parameters used are $v_F = 0.5 \times 10^6$ m s⁻¹, $\Delta_h = 20$ meV, and $\Delta_\Omega = 30$ meV ($e v_F A_0 = 0.48$ eV, $\hbar \Omega = 7.5$ eV) [18]. The $n = 0$ LL appears in the hole band for right-handed light (red curves, $l = 1$) and in the electron band for left-handed light (black curves, $l = -1$), see figure 1. The exchange of surface states induced by the field B and the *off-resonant* light in such FTIs is an entirely new phenomenon. The energies of the two surfaces are different for $B \rightarrow 0$, since the gap $l\Delta_\Omega \pm \Delta_h$ increases for one surface and decreases for the other.

We emphasize that the band gaps $l\Delta_\Omega + s\Delta_h$ at the two surfaces of ultrathin FTIs can be made different by, e.g. varying the light's frequency or amplitude. This can create, e.g. for $l = 1$, one surface with a small gap $\Delta_\Omega - \Delta_h$ and the other one with a large gap $\Delta_\Omega + \Delta_h$; for $l = -1$ these gaps could be exchanged. Accordingly, only the antisymmetric or symmetric surface contributes to the transport properties depending on the light polarization ($l = \pm 1$). Such a situation could be realized in experiments on FTIs, similar to those of [23, 24], by varying the sample thickness [29] down to the limit of 6 nm below which different energies Δ_h have been reported [29]. To our knowledge this is a novel state of matter in FTIs like Bi₂Se₃, Bi₂Te₃, HgTe, and related materials.

Longitudinal conductivity

For weak scattering potentials the current is due to hopping between orbit centres as a result of carrier collisions with, e.g. charged impurities [25]. In a normal magnetic field the diffusive contribution $\sigma_{xx}^{\text{diff}}$ to σ_{xx} vanishes and only the collisional contribution $\sigma_{xx}^{\text{col}} \equiv \sigma_{xx}$ is important; it is given by [25, 26]

$$\sigma_{xx} = \frac{e^2 \beta}{2S_0} \sum_{\zeta \neq \zeta'} f(E_\zeta) [1 - f(E_{\zeta'})] W_{\zeta\zeta'} (X_\zeta - X_{\zeta'})^2, \quad (4)$$

where $f(E_\zeta) = (\exp[\beta(E_\zeta - E_F)] + 1)^{-1}$ is the Fermi Dirac distribution function, $\beta = k_B T$, T the temperature, k_B the Boltzmann constant, and E_F the Fermi energy. $W_{\zeta\zeta'}$ is the transition rate between the one-electron states $|\zeta\rangle$ and $|\zeta'\rangle$, and e the charge of the electron. Here $f(E_\zeta) = f(E_{\zeta'})$ for elastic scattering and $X_\zeta = \langle \zeta | x | \zeta \rangle$ with x being the position operator.

The scattering rate is given by Fermi's golden rule

$$W_{\zeta\zeta'} = F \sum_{\zeta \neq \zeta'} |U(\mathbf{q})|^2 |J_{\zeta\zeta'}(u)|^2 \delta(E_\zeta - E_{\zeta'}) \delta_{k_x, k'_x + q_x}, \quad (5)$$

with $F = 2\pi N_i / S_0 \hbar$, $q^2 = q_x^2 + q_y^2$, $u = l_B^2 q^2 / 2$, and N_i the impurity density. $J_{\zeta\zeta'}(u) = \langle \zeta | \exp(i\mathbf{q} \cdot \mathbf{r}) | \zeta' \rangle$ are the form factors and $|\zeta\rangle \equiv |n, s, l, k_y\rangle$. $U(\mathbf{q}) = U_0 / (q^2 + k_s^2)^{1/2}$ with $U_0 = e^2 / (2\epsilon_r \epsilon_0)$. Further, k_s is the screening wave vector, ϵ_r the relative permittivity, and ϵ_0 the permittivity of the vacuum. Furthermore, if the impurity potential is short-ranged (of the Dirac δ -function type), one may use the approximation $k_s \gg q$ and obtain $U(\mathbf{q}) \approx U_0 / k_s$. Since the scattering is elastic and the eigenfunctions are degenerate in the quantum number k_x , see equation (3), only the $n \rightarrow n$ transitions are allowed. Further, we have $(X_\zeta - X_{\zeta'})^2 = l_B^4 q_y^2$, transform the sums over k_y and q into integrals, and evaluate them using cylindrical coordinates. The form factor $|J_{\zeta\zeta'}(u)|^2$ can be evaluated from the matrix element $\langle \zeta | \exp(i\mathbf{q} \cdot \mathbf{r}) | \zeta' \rangle$. The result is $|J_{mm}(u)|^2 = \exp(-u) (|C_{n,s}^{\lambda,l}|^2 L_n(u) + |D_{n,s}^{\lambda,l}|^2 L_{n-1}(u))^2$ for $n = n'$. With these details equation (4) takes the form

$$\sigma_{xx} = \frac{e^2}{h} \frac{N_i \beta U_0^2}{4u_{sc} \hbar \omega_c} \sum_{s,n} I_{n,s}^{\lambda,l} f(E_{n,s}^{\lambda,l}) [1 - f(E_{n,s}^{\lambda,l})], \quad (6)$$

where $f(E_{n,s}^{\lambda,l}) = (\exp[\beta(\lambda[\hbar^2 \omega_c^2 n + (\Delta_{s,l})^2]^{1/2} - E_F)] + 1)^{-1}$ and $u_{sc} = l_B^2 k_s^2 / 2$. The sum over s is trivial since the two surfaces can be treated independently due to the different gaps. The factor $I_{n,s}^{\lambda,l}$ in equation (6) is the integral $\int_0^\infty u |J_{mm}(u)|^2 du$ that can be evaluated analytically using the properties of the orthogonal polynomials $L_n(u)$. The result is

$$I_{n,s}^{\lambda,l} = (2n+1) |C_{n,s}^{\lambda,l}|^4 - 2n |C_{n,s}^{\lambda,l}|^2 |D_{n,s}^{\lambda,l}|^2 + (2n-1) |D_{n,s}^{\lambda,l}|^4. \quad (7)$$

For $\Delta_{s,l} = 0$, equation (7) reduces to $2n/4$, which means that the minima of σ_{xx} occur at the odd factors $\nu = 2n+1$ in accord with [26].

Since the band gap $l\Delta_\Omega + s\Delta_h$ becomes surface dependent, see figure 1, the longitudinal conductivity is dominated by one surface only, that of the symmetric or antisymmetric surface states. As usual, this conductivity, given by equation (6), exhibits Shubnikov-de Haas oscillations. For $\Delta_h = \Delta_\Omega = 0$ we must consider both surfaces. The electron-hole spectrum is symmetric with a single peak (solid curve) at the Dirac point, as shown in figure 2(a), using the parameters

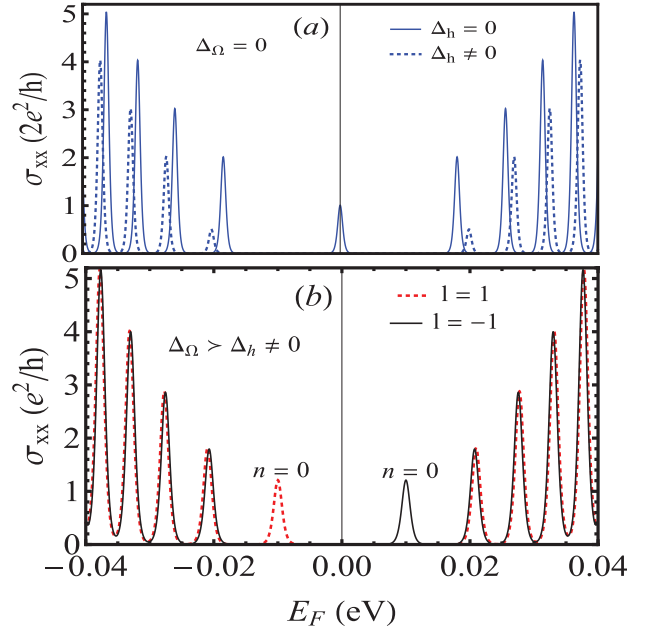


Figure 2. Longitudinal conductivity as a function of the Fermi energy E_F for $T = 2$ K and $B = 1$ T. (a) The solid curve is for $\Delta_\Omega = \Delta_h = 0$ meV and the dashed one for $\Delta_h = 20$ meV and $\Delta_\Omega = 0$ meV. (b) The red dashed curve is for antisymmetric ($s = -1$) surface states with right-handed light and the black solid one for symmetric ($s = 1$) surface states with left-handed light with $\Delta_h = 20$ meV and $\Delta_\Omega = 30$ meV.

[6–8]: $N_i = 1 \times 10^{13} \text{ m}^{-2}$, $\mu_B = 5.788 \times 10^{-5} \text{ eV T}^{-1}$, $T = 2$ K, $B = 1$ T, $k_s = 10^{-7} \text{ m}^{-1}$, $v_F = 5 \times 10^5 \text{ m s}^{-1}$, and $\epsilon_r = 4$. We find a gap Δ_h at the Dirac point for $\Delta_h \neq 0$ and $\Delta_\Omega = 0$ with symmetric electron-hole behaviour (dashed curve). This gives $\sigma_{xx} = 0$ at the Dirac point and the peak at $E_F = 0$ (solid curve) splits into two peaks, one in the electron ($s = -1$) and one in the hole band ($s = 1$) in accord with equation (2).

For $\Delta_\Omega > \Delta_h > 0$ the electron-hole spectrum is asymmetric and we consider only one surface depending on the light's polarization. We consider only the symmetric surface states ($s = 1$, black curves) for left-handed light ($l = -1$) or the antisymmetric surface states ($s = -1$, red curves) for right-handed light ($l = 1$) and show σ_{xx} in figure 2(b). As seen, the $n = 0$ LL shifts into the hole or electron band. The shift can be understood with the help of the eigenvalues shown in figure 1: for right-(left-)handed light the $n = 0$ LL moves into the hole (electron) band. This is a nontrivial state entirely new in FTIs. We notice in passing that were we to plot the current polarization $P = [\sigma_{xx}(l = 1) - \sigma_{xx}(l = -1)] / [\sigma_{xx}(l = 1) + \sigma_{xx}(l = -1)]$ we would have, on account of figure 2(b), only two peaks of height $P = 1$ (-1) centred at $E_F \approx -0.01$ (0.01) eV. Also, had we considered the $s = -1$ surface with left-handed light ($l = -1$) or the $s = 1$ surface with right-handed light ($l = 1$), σ_{xx} would be zero in the entire range of figure 2 since the corresponding surface states start at ± 0.05 eV, see figure 1 for $B = 1$ T. This is also corroborated by the fact that at very low temperatures the factor $\beta f(\dots)[1 - f(\dots)]$ in equation (6) behaves as the function $\delta(E_{n,s}^{\lambda,l} - E_F)$.

Hall conductivity

For linear responses to a weak source-to-drain electric field, the Hall conductivity is given by the Kubo–Greenwood formula [25, 26]

$$\sigma_{\mu\nu} = \frac{i\hbar e^2}{S_0} \sum_{\zeta \neq \zeta'} \frac{(f_{\zeta} - f_{\zeta'}) v_{\nu\zeta\zeta'} v_{\mu\zeta'\zeta}}{(E_{\zeta} - E_{\zeta'})(E_{\zeta} - E_{\zeta'} + i\Gamma_{\zeta})}, \quad (8)$$

where $v_{\nu\zeta\zeta'}$ and $v_{\mu\zeta'\zeta}$ are the nondiagonal matrix elements of the velocity operator with $\mu = x, y, \nu = x, y$. The sum runs over all quantum numbers of the states $|\zeta\rangle \equiv |n, s, l, k_y\rangle$ and $|\zeta'\rangle \equiv |n', s', l', k'_y\rangle$ provided $\zeta \neq \zeta'$. Assuming that the level broadening is approximately the same for all LLs, $\Gamma_{\zeta} = \Gamma$, one can show that the imaginary part of equation (8) vanishes. To obtain the most transparent results for the Hall conductivity σ_{yx} , we take $\Gamma = 0$. The relevant velocity matrix elements are obtained from equation (1), for $\nu = x$ and $\mu = y$, and the evaluation follows the procedure detailed in [26]. The result for σ_{yx} can be expressed as a sum of two terms, one (*I*) for $n \geq 1$ and the other (*II*) for $n = 0$, i.e. $\sigma_{yx} = \sigma_{yx}^I + \sigma_{yx}^{II}$, with

$$\sigma_{yx}^I = \frac{e^2}{h} \sum_{s,n=1}^{\infty} \left\{ (n + 1/2) [f_{n,s}^{+,l} - f_{n+1,s}^{+,l} + f_{n,s}^{-,l} - f_{n+1,s}^{-,l}] - \frac{\Delta_{s,l}}{2} \left[\frac{f_{n,s}^{+,l} - f_{n,s}^{-,l}}{E_{n,s}^{+,l}} - \frac{f_{n+1,s}^{+,l} - f_{n+1,s}^{-,l}}{E_{n+1,s}^{+,l}} \right] \right\}. \quad (9)$$

The sum over n starts at $n = 1$, because the $n = 0$ LL is treated separately. That over s is trivial, as we consider only one surface at a time. For $n = 0$ equation (8) gives

$$\sigma_{yx}^{II} = \frac{e^2}{h} \sum_s \{ f_{0,s}^{+,l} + f_{0,s}^{-,l} - (f_{1,s}^{+,l} + f_{1,s}^{-,l})/2 + \Delta_{s,l} (f_{1,s}^{+,l} - f_{1,s}^{-,l})/2E_{1,s}^{+,l} \}. \quad (10)$$

At zero or very low temperature the sum over s in equations (9) and (10) has the value 1 for $n = n_F$, since for a single surface the number of filled states is 1. Here n_F is the LL index at the Fermi energy. Notice also that for $\Delta_{s,l} = 0$ equations (9) and (10) take the form $\sigma_{yx} = 2(e^2/h)(n + 1/2)$ or in terms of the filling factor $\nu = 2(n + 1/2)$ as $\sigma_{yx} = \nu e^2/h$ for TIs [6–8, 30]. An important aspect in the QHE in graphene, TIs, silicene, MoS₂, etc is the LL at zero energy (gapless graphene) or its modification in gapped systems.

Similar to the band structure and longitudinal conductivity, the unconventional QHE is dominated by one surface. That is, only the symmetric or antisymmetric surface contributes to it for left- or right-handed light, respectively. We show the Hall conductivity σ_{yx} in figure 3, for $s = 1$, as a function of E_F . In the limit $\Delta_{s,l} \rightarrow 0$ ((a), solid curve) these results reduce to an odd-integer QHE in TIs by multiplying with a factor 2 for surface degeneracy [6, 30] (limit of zero strain in [8]), where the plateaus appear at $(\pm 1, \pm 3, \pm 5, \dots)e^2/h$, and both surfaces must be considered as in the case of figure 2(a). The results of figure 3(a), dashed curve, can be reduced to those

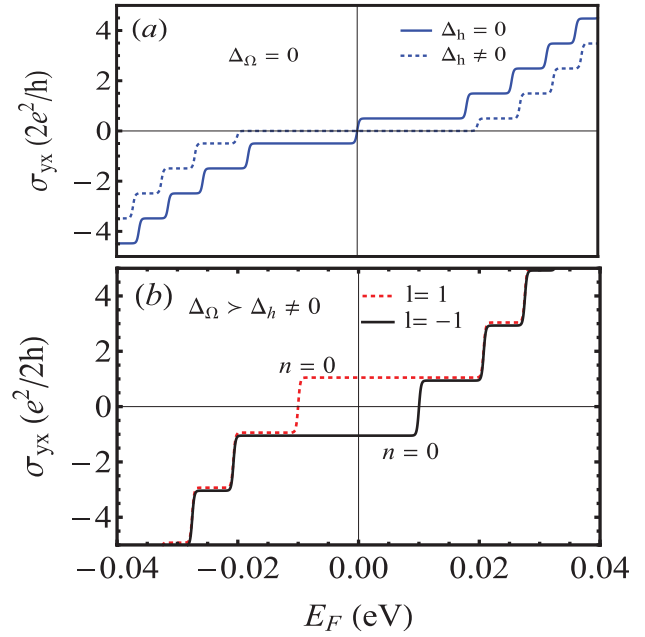


Figure 3. Hall conductivity versus Fermi energy E_F . All curves, marked as in figure 2, are obtained with the same parameters.

of single-valley gapped graphene for $\Delta_h \neq 0$ [26], irrespective of a factor of 2 due to valley degeneracy, and to those of gapped TIs [31]. However, for $\Delta_{\Omega} > \Delta_h \neq 0$ only one surface must be considered, see figure 2(b) for σ_{xx} . The Hall plateaus occur at half-integer values in contrast to previous results for graphene and TIs, as shown in figure 3(b). At the Dirac point we have $\sigma_{yx} = e^2/2h$ for right-handed light (dashed curve) and $\sigma_{yx} = -e^2/2h$ for left-handed light (solid curve), due to the occurrence of the $n = 0$ LL in the hole and electron band, respectively. Again, had we considered the $s = -1$ surface with left-handed light or the $s = 1$ surface with right-handed light, σ_{yx} would vanish in the E_F range of figure 3, since the corresponding states would start at ± 0.05 eV and the occupation factors $f(\dots)$ would be zero.

The electron–hole symmetry is broken and the plateaus appear at $(\pm 1/2, \pm 3/2, \pm 5/2, \dots)e^2/h$. This shows a nontrivial transition at the Dirac point which could be experimentally tested. It occurs because the energy term Δ_{Ω} due to the *off-resonant* light at the Dirac point can be externally tuned to higher values [23, 24]. As for the influence of level broadening, i.e. finite Γ , on the results, on the basis of [26] we strongly expect they will not be altered qualitatively. After all, the QHE has already been realized on TIs [8]. These signatures of novel quantum phase transitions in FTIs are distinct from those in graphene or in TIs without light and relate to different values of the Hall conductivity. They could be tested in experiments similar to those performed on semiconducting silicon [32, 33]. Moreover, radiation effects and light-dependent magnetotransport have been observed for Dirac fermions in the presence of *on-resonant* light [34, 35]. Accordingly, we believe our results can be tested in similar experiments using *off-resonant* light [23, 24], a regime that is different from that of the optical absorption spectra [15, 36].

Summary

We have identified an unconventional QHE in FTIs, in the presence of a perpendicular magnetic field, by evaluating their band structure and the Hall and longitudinal conductivities. The low-energy dynamics can be governed by a single-surface in a wide range of Fermi energies. This results in a nontrivial phase transition and unusual Hall plateaus at *half-integer* multiples of e^2/h ($\pm 1/2, \pm 3/2, \pm 5/2, \dots$). In addition, reversing the light polarization leads to an exchange of surface states, in both the valence and conduction bands, and to a shift of the $n = 0$ LL into the hole and electron bands, respectively. These findings suggest new directions in experimental research and device applications based on FTIs.

Acknowledgments

This work was supported by the Canadian NSERC Grant No. OGP0121756 (MT, PV). The research reported in this publication was supported by funding from King Abdullah University of Science and Technology (KAUST) (US).

References

- [1] Novoselov K S, Geim A K, Morozov S V, Jiang D, Katsnelson M I, Grigorieva I V, Dubonos S V and Firsov A A 2005 *Nature* **438** 197
- [2] Zhang Y, Tan Y-W, Stormer H L and Kim P 2005 *Nature* **438** 201
- [3] Gusynin V P and Sharapov S G 2005 *Phys. Rev. Lett.* **95** 146801
- [4] Tahir M and Schwingenschlöggl U 2013 *Sci. Rep.* **3** 1075
- [5] Shakouri Kh, Vasilopoulos P, Vargiamidis V and Peeters F M 2014 *Phys. Rev. B* **90** 235423
- [6] Li X, Zhang F and Niu Q 2013 *Phys. Rev. Lett.* **110** 066803
- [7] Cui X *et al* 2015 *Nat. Nanotechnol.* **10** 534
- [8] Wang X F and Vasilopoulos P 2003 *Phys. Rev. B* **67** 085313
- [9] Qu D-X, Hor Y S, Xiong J, Cava R J and Ong N P 2010 *Science* **329** 821
- [10] Cheng P *et al* 2010 *Phys. Rev. Lett.* **105** 076801
- [11] Yang Z and Han J H 2011 *Phys. Rev. B* **83** 045415
- [12] Chu R-L, Shi J and Shen S-Q 2011 *Phys. Rev. B* **84** 085312
- [13] Li H, Sheng L and Xing D Y 2011 *Phys. Rev. B* **84** 035310
- [14] Vafek O 2011 *Phys. Rev. B* **84** 245417
- [15] Zuzin A A and Burkov A A 2011 *Phys. Rev. B* **83** 195413
- [16] Sitte M, Rosch A, Altman E and Fritz L 2012 *Phys. Rev. Lett.* **108** 126807
- [17] Brune C, Liu C X, Novik E G, Hankiewicz E M, Buhmann H, Chen Y L, Qi X L, Shen Z X, Zhang S C and Molenkamp L W 2011 *Phys. Rev. Lett.* **106** 126803
- [18] Cao H, Tian J, Miotkowski I, Shen T, Hu J, Qiao S and Chen Y P 2012 *Phys. Rev. Lett.* **108** 216803
- [19] Xu Y, Miotkowski I, Liu C, Tian J, Nam H, Alidoust N, Hu J, Shih C-K, Hasan M Z and Chen Y P 2014 *Nat. Phys.* **10** 956
- [20] Hasan M Z and Kane C L 2010 *Rev. Mod. Phys.* **82** 3045
- [21] Qi X L and Zhang S-C 2011 *Rev. Mod. Phys.* **83** 1057
- [22] König M, Wiedmann S, Brune C, Roth A, Buhmann H, Molenkamp L W, Qi X-L and Zhang S-C 2007 *Science* **318** 766
- [23] Bernevig B, Hughes T A and Zhang S-C 2006 *Science* **314** 1751
- [24] Zhang H, Liu C-X, Qi X-L, Dai X, Fang Z and Zhang S-C 2009 *Nat. Phys.* **5** 438
- [25] Hsieh D *et al* 2009 *Nature* **460** 1101
- [26] Sakamoto Y, Hirahara T, Miyazaki H, Kimura S-I and Hasegawa S 2010 *Phys. Rev. B* **81** 165432
- [27] Linder J, Yokoyama T and Sudbo A 2009 *Phys. Rev. B* **80** 205401
- [28] Fu Y-S, Kawamura M, Igarashi K, Takagi H, Hanaguri T and Sasagawa T 2014 *Nat. Phys.* **10** 815
- [29] Pertsova A, Canali C M and MacDonald A H 2015 *Nat. Phys.* **91** 075430
- [30] Kitaev A and Preskill J 2006 *Phys. Rev. Lett.* **96** 110404
- [31] Moore J E 2010 *Nature* **464** 194
- [32] Efimkin D K and Lozovik Y E 2013 *Phys. Rev. B* **87** 245416
- [33] Li Z and Carbotte J P 2013 *Phys. Rev. B* **88** 045414
- [34] Lasia M and Brey L 2014 *Phys. Rev. B* **90** 075417
- [35] Zhang X, Wang J and Zhang S-C 2010 *Phys. Rev. B* **82** 245107
- [36] Linder N H, Refael G and Galitski V 2011 *Nat. Phys.* **7** 490
- [37] Kitagawa T, Oka T, Brataas A, Fu L and Demler E 2011 *Phys. Rev. B* **84** 235108
- [38] Narayan A 2015 *Phys. Rev. B* **91** 205445
- [39] Dahlhaus J P, Fregoso B M and Moore J E 2015 *Phys. Rev. Lett.* **114** 246802
- [40] Dehghani H, Oka T and Mitra A 2015 *Phys. Rev. B* **91** 155422
- [41] Sacramento P D 2015 *Phys. Rev. B* **91** 214518
- [42] Gu Z, Fertig H A, Arovas D P and Auerbach A 2011 *Phys. Rev. Lett.* **107** 216601
- [43] Ezawa M 2013 *Phys. Rev. Lett.* **110** 026603
- [44] Gómez-León Á, Deplace P and Platero G 2014 *Phys. Rev. B* **89** 205408
- [45] Zhai X and Jin G 2014 *Phys. Rev. B* **89** 235416
- [46] Rechtsman M C, Zeuner J M, Plotnik Y, Lumer Y, Podolsky D, Dreisow F, Nolte S, Segev M and Szameit A 2013 *Nature* **496** 196
- [47] Wang Y H, Steinberg H, Herrero P J and Gedik N 2013 *Science* **342** 453
- [48] Zhang H, Yao J, Shao J, Li H, Li S, Bao D, Wang C and Yang G 2014 *Sci. Rep.* **4** 5876
- [49] Charbonneau M, Van Vliet K M and Vasilopoulos P 1982 *J. Math. Phys.* **23** 318
- [50] Vasilopoulos P 1985 *Phys. Rev. B* **32** 771
- [51] Krstajić P M and Vasilopoulos P 2011 *Phys. Rev. B* **83** 075427
- [52] Krstajić P M and Vasilopoulos P 2012 *Phys. Rev. B* **86** 115432
- [53] Lu H-Z, Shan W-Y, Yao W, Niu Q and Shen S-Q 2010 *Phys. Rev. B* **81** 115407
- [54] Tahir M and Vasilopoulos P 2015 *Phys. Rev. B* **91** 115311
- [55] Zhang Y *et al* 2010 *Nat. Phys.* **6** 584
- [56] Analytis J G, McDonald R D, Riggs S C, Chu J-H, Boebinger G S and Fisher I R 2010 *Nat. Phys.* **6** 960
- [57] Büttner B *et al* 2011 *Nat. Phys.* **7** 418
- [58] Tabert C J and Carbotte J P 2015 *Phys. Rev. B* **91** 235405
- [59] Arnone D D, Frost J E F, Smith C G, Ritchie D A, Jones G A C, Butcher R J and Pepper M 1995 *Appl. Phys. Lett.* **66** 3149
- [60] Karch J, Tarasenko S A, Ivchenko E L, Kamann J, Olbrich P, Utz M, Kvon Z D and Ganichev S D 2011 *Phys. Rev. B* **83** 121312
- [61] Olbrich P *et al* 2013 *Phys. Rev. B* **87** 235439
- [62] Karch J *et al* 2010 *Phys. Rev. Lett.* **105** 227402
- [63] Tse W-K and MacDonald A H 2011 *Phys. Rev. B* **84** 205327
- [64] Garate I and Franz M 2011 *Phys. Rev. B* **84** 045403